

1      **Molecular phylogenetics supports a clade of red algal parasites retaining native**  
2                                      **plastids: taxonomy and terminology revised**

3

4                                      *Eric D. Salomaki<sup>1,2</sup> and Christopher E. Lane<sup>1</sup>*

5

6      <sup>1</sup>Department of Biological Sciences, University of Rhode Island, Kingston, RI, USA.

7

8

9

10

11      Running head: Biological basis for defining red algal parasites

12

13      Author for correspondence: email [eric.salomaki@gmail.com](mailto:eric.salomaki@gmail.com)

14      <sup>2</sup>Present address: Institute of Parasitology, Biology Centre, Czech Academy of Science,

15      České Budějovice, Czech Republic 370 05

16

17 **Abstract:**

18 Parasitism is a life strategy that has repeatedly evolved within the  
19 Florideophyceae. Historically, the terms adelphoparasite and alloparasite have been used  
20 to distinguish parasites based on the relative phylogenetic relationship of host and  
21 parasite. However, analyses using molecular phylogenetics indicate that nearly all red  
22 algal parasites infect within their taxonomic family, and a range of relationships exist  
23 between host and parasite. To date, all investigated adelphoparasites have lost their  
24 plastid, and instead, incorporate a host derived plastid when packaging spores. In  
25 contrast, a highly reduced plastid lacking photosynthesis genes was sequenced from the  
26 alloparasite *Choreocolax polysiphoniae*. Here we present the complete *Harveyella*  
27 *mirabilis* plastid genome, which has also lost genes involved in photosynthesis, and a  
28 partial plastid genome from *Leachiella pacifica*. The *H. mirabilis* plastid shares more  
29 synteny with free-living red algal plastids than that of *C. polysiphoniae*. Phylogenetic  
30 analysis demonstrates that *C. polysiphoniae*, *H. mirabilis*, and *L. pacifica* form a robustly  
31 supported clade of parasites, which retain their own plastid genomes, within the  
32 Rhodomelaceae. We therefore transfer all three genera from the exclusively parasitic  
33 family, Choreocolacaceae, to the Rhodomelaceae. Additionally, we recommend applying  
34 the terms archaeplastic parasites (formerly alloparasites), and neoplastic parasites  
35 (formerly adelphoparasites) to distinguish red algal parasites using a biological  
36 framework rather than taxonomic affiliation with their hosts.

37

38 **Keywords:** Alloparasite, Adelphoparasite, *Choreocolax*, *Harveyella*, *Leachiella*,  
39 Choreocolacaceae, Rhodomelaceae

- 40 **Abbreviations:** ORF = Open Reading Frame; BI = Bayesian inference; MCMCMC =  
41 Metropolis-coupled Markov chain Monte Carlo

42 **INTRODUCTION:**

43           Since the late 19<sup>th</sup> century when parasitic red algae were first formally recognized  
44 the number of red algal parasite species has been steadily increasing (Reinsch 1875,  
45 Setchell 1914, 1923, Goff 1982, Preuss et al. 2017). Recent counts identify 124 distinct  
46 species of red algal parasites distributed across eight of the 31 of the Florideophyceae  
47 (Salomaki and Lane 2014, Blouin and Lane 2015, Preuss et al. 2017, Preuss and  
48 Zuccarello 2018, Guiry and Guiry 2018). The abundance of successful independent  
49 evolutions of parasitism within the Florideophyceae seems in large part due to their  
50 ability to form direct cell-to-cell fusions between adjacent, non-daughter cells  
51 (Wetherbee and Quirk 1982a, Goff and Coleman 1985). With few exceptions [e.g.  
52 *Choreonema thuretii* (Broadwater and LaPointe 1997)], red algal parasites use their  
53 ability to form cell fusions as a means of infecting their host (Goff and Coleman 1985,  
54 Zuccarello et al. 2004).

55           Red algal parasites exclusively infect other rhodophytes and are predominately  
56 unpigmented, appearing as galls or irregular growths on their free-living red algal hosts.  
57 Despite their diminutive habit, parasitic red algae share morphological characteristics  
58 with other close relatives, and thus were assigned to tribes or families at the time of their  
59 initial discovery (Reinsch 1875, Feldmann and Feldmann 1958). In the early 20<sup>th</sup> century,  
60 two hypotheses arose to explain the origins of red algal parasites. First, Setchell (1918)  
61 noted that approximately 80% of the parasites he was studying infected hosts in the same  
62 family. Based upon his observations, he proposed that parasites originated as carpospores  
63 or tetraspores of their host, which had undergone a mutation causing reduced  
64 photosynthetic capabilities (Setchell 1918). Later, Sturch (1926) proposed that rather than

65 evolving sympatrically, parasitic red algae started out as small epiphytes of their hosts  
66 that eventually would penetrate cortical cells of the host, becoming an endophyte. Once  
67 established as an endophyte, the alga would adopt mechanisms to obtain nutrients from  
68 the host, becoming increasingly reliant on its host, solidifying an irreversible path  
69 towards parasitism (Sturch 1926). Feldmann and Feldmann (1958) furthered Sturch's  
70 hypothesis, adding that epiphytes that are closely related to their hosts are more likely to  
71 succeed in creating connections with hosts cells and are therefore more likely to complete  
72 a transition to parasitism.

73         Historically parasites that have infected species within their own family or tribe  
74 have been considered 'adelphoparasites', while those more distantly related to their hosts  
75 are called 'alloparasites' (Feldmann and Feldmann 1958, Goff et al. 1996). In agreement  
76 with Setchell's initial observations (1918), approximately 80% of the currently described  
77 red algal parasite species are considered to be adelphoparasitic, while the remaining 20%  
78 are alloparasitic (Goff 1982, Salomaki and Lane 2014, Blouin and Lane 2015). Based  
79 initially on morphological observations, and later coupled with molecular data, it was  
80 proposed that parasites evolve sympatrically with their hosts, as adelphoparasites, and  
81 over time diversify or adapt to infect new and more distantly related hosts, becoming  
82 alloparasites (Feldmann and Feldmann 1958, Blouin and Lane 2012).

83         Sturch (1926) described the Choreocolacaceae as a family in the Gigartinales  
84 comprised of morphologically reduced parasites lacking chlorophyll including species of  
85 *Choreocolax*, *Harveyella*, and *Holmsella*. This exclusively parasitic family was the  
86 subject of a thorough phylogenetic analysis of alloparasites to confirm whether these  
87 parasitic red algae were truly monophyletic (Zuccarello et al. 2004). Their study

88 supported previous morphological observations (Fredericq and Hommersand 1990)  
89 confirming that *Holmsella* was a member of the Gracilariaceae and questioned the  
90 legitimacy of recognizing a family of red algal parasites. However, Zuccarello et al.  
91 (2004) did not formally address the taxonomic implications for the Choreocolacaceae.

92 In the few other cases where molecular phylogenetics have been applied to assess  
93 evolutionary histories of red algal parasites, data suggests that red algal parasites have  
94 arisen through numerous independent evolutionary events (Goff et al. 1996, 1997,  
95 Kurihara et al. 2010). In addition to phylogenetic analyses, molecular tools have also  
96 been applied to investigate the parasite-host dynamics throughout parasite development.  
97 Analyses of the adelphoparasites *Gardneriella tuberifera* Kylin, *Gracilariophila*  
98 *oryzoides* Setchell & H. L. Wilson demonstrated that, although the parasites maintain a  
99 native mitochondrion, they have lost their native plastid and instead ‘hijack’ a host plastid  
100 when packaging their own spores (Goff and Coleman 1995). To date, all red algal  
101 parasites examined maintain a fully functional mitochondrion (Salomaki and Lane 2016).  
102 All adelphoparasites that have been investigated have lost their native plastid (Goff and  
103 Coleman 1995; Salomaki and Lane 2014), and next-generation sequencing efforts  
104 targeting *Faucheocolax attenuatus* Setchell, *Janczewskia gardneri* Setchell & Guernsey,  
105 and *G. oryzoides* support these findings (Salomaki and Lane unpublished). In contrast, a  
106 highly reduced native plastid was sequenced from the alloparasite *Choreocolax*  
107 *polysiphoniae* Reinsch, which lost genes involved in photosynthesis, yet maintains  
108 functions including fatty acid and amino acid biosynthesis (Salomaki et al. 2015). The  
109 lack of plastids in adelphoparasites, in combination with finding a native plastid in the

110 alloparsite *C. polysiphoniae*, demonstrates that not all parasites pass through an  
111 ‘adelphoparasite stage’ and that there are multiple paths to parasitism in red algae.

112 In their study examining relationships in the Choreocolacaceae, Zuccarello *et al.*  
113 (2004) found that *Holmsella pachyderma* and *Holmsella australis* formed a clade within  
114 the Gracilariaceae. Additionally they demonstrated that the parasite genera *Choreocolax*,  
115 *Harveyella*, and *Leachiella* belonged in the Rhodomelaceae, but lacked support for a  
116 monophyletic group of parasites. Using DNA sequence data we investigated the  
117 relationships of *Choreocolax*, *Harveyella*, and *Leachiella*, and tested the hypothesis that  
118 parasites can arise and subsequently speciate, forming clades that infect a range of hosts.  
119 Furthermore, we explored the evolution of parasitism and the loss of photosynthesis  
120 among species traditionally called alloparsites.

121

## 122 **MATERIALS AND METHODS**

### 123 *Sample Collection and DNA Extraction*

124 *Harveyella mirabilis* (Reinsch) F.Schmitz & Reinke, on its host, *Odonthalia*  
125 *washingtoniensis* Kylin, was collected from Cattle Point, Friday Harbor, WA, USA  
126 (48.452428, -122.962774), and *Leachiella pacifica* Kugrens, on *Polysiphonia hendryi*  
127 N.L. Gardner, was collected off the dock at Friday Harbor Laboratories, Friday Harbor  
128 WA, USA (48.545066, -123.012268). Individual parasite galls from *Harveyella mirabilis*  
129 and *Leachiella pacifica* were dissected from their respective hosts and collected in a 1.5  
130 mL microcentrifuge tube. Unfortunately, only single parasites of *H. mirabilis* and *L.*  
131 *pacifica* were observed on the host tissue and the entire pustule was excised for DNA  
132 isolation. Dried vouchers for the remaining host tissue from *Polysiphonia hendryi*

133 (specimen 03304646) and *Odonthalia washingtoniensis* (specimen 03304647) have been  
134 deposited at the New York Botanical Garden herbarium (NY). Parasite tissue was hand-  
135 ground using a Corning Axygen® PES-15-B-SI disposable tissue grinder pestle in a 1.5  
136 mL microcentrifuge tube while submerged in 100µL of DNA extraction buffer (Saunders  
137 1993). DNA was extracted from specimens using a standard phenol/chloroform  
138 extraction with all ratios adjusted for an initial buffer volume of 100µL (Saunders 1993).  
139

#### 140 *Molecular Analyses*

141 Genomic DNA was amplified from *Harveyella mirabilis* and *Leachiella pacifica*  
142 using the illustra Single Cell GenomiPhi DNA Amplification kit (GE Healthcare Life  
143 Sciences, Pittsburgh, Pa) according to manufacturer protocols. Libraries for Illumina  
144 sequencing were constructed from the amplified DNA on the Apollo 324 robot using the  
145 PrepX ILM DNA Library Kit (Wafergen Biosystems, Fremont, CA, USA). The  
146 *Harveyella mirabilis* and *Leachiella pacifica* libraries were multiplexed and sequenced  
147 on an Illumina MiSeq paired-end 250 x 250 basepair run. The sequencing effort resulted  
148 in 7,923,094 paired end reads for *Harveyella mirabilis* and 7,502,360 paired-end reads  
149 for *Leachiella pacifica*. Raw sequencing reads with Phred scores <30 were removed and  
150 the remaining reads were trimmed of adapter sequences. Additionally, fifteen 5' and five  
151 3' nucleotides were trimmed from the remaining reads and all reads under 100  
152 nucleotides were removed from the dataset. All trimming was completed using CLC  
153 Genomics Workbench v. 9.5.2 (CLC Bio-Qiagen, Aarhus, Denmark) and the remaining  
154 reads were assembled using default parameters in CLC Genomics Workbench v. 9.5.2.  
155



156 *Plastid Genome Annotation*

157 A 90,654 bp contig was identified as the plastid genome of *Harveyella mirabilis*  
158 from the assembled Illumina MiSeq data (GenBank Accession MK039118). We  
159 recovered >40,000 bp of the *Leachiella pacifica* plastid genome that were in five separate  
160 contigs (GenBank Accession MK039114-MK039117, MK039119). Open reading frame  
161 (ORF) prediction on the plastid genomes was done in Geneious Pro v. 9.1.5 and the  
162 resulting ORFs were manually annotated using GenBank and Pfam (Finn et al. 2010,  
163 2015) databases. Functional annotations were assigned from the UniProt (The UniProt  
164 Consortium 2017) and KEGG databases (Kanehisa et al. 2016). Genes found in red algal  
165 plastid genomes that were missing from the *H. mirabilis* plastid were searched for using  
166 BLAST, against the plastid sequence and the genomic assemblies to verify their absence  
167 and check for evidence of transfer to another genetic compartment. Plastid genome  
168 sequences were submitted to the tRNAscan-SE online server v1.21 (Schattner et al. 2005)  
169 for identification of tRNA sequences and to MFannot  
170 (<http://megasun.bch.umontreal.ca/cgi-bin/mfannot/mfannotInterface.pl>) to identify rRNA  
171 sequences and confirm manual gene annotations.

172

173 *Plastid Genome Comparative Analysis*

174 The circular plastid genomes of from the florideophytes, *Calliarthron*  
175 *tuberculosis* (KC153978), *Ceramium cimbricum* (KR025491), *Ceramium japonicum*  
176 (KX284719), *Chondrus crispus* (HF562234), *Dasya binghamiae* (KX247284), *Laurencia*  
177 *sp.* JFC0032 (LN833431), *Grateloupia taiwanensis* (KC894740), *Gracilaria*  
178 *tenuistipitata* (AY673996), *Vertebrata lanosa* (KP308097), and the alloparasites

179 *Choreocolax polysiphoniae* (KP308096) and *Harveyella mirabilis* (MK039118) were  
180 arranged so that their sequences began with the *ftsH* gene. Whole genome alignment was  
181 completed using the default settings for the progressiveMauve algorithm in the Mauve  
182 v2.3.1 (Darling et al. 2004).

183

#### 184 *Phylogenetic Analysis*

185 A data matrix comprising 17 protein coding genes (*accB*, *acpP*, *fabH*, *ilvH*, *odpA*,  
186 *rne*, *rpl16*, *rpl20*, *rpl3*, *rps14*, *rps16*, *rps19*, *sufB*, *trpA*, *trpG*, *tsf*, *ycf19*) and two plastid  
187 encoded rRNAs (*rnl*, *rns*) that were shared between the *Harveyella mirabilis* plastid, the  
188 partial *Leachiella pacifica* plastid, and 55 completely sequenced plastid genomes from  
189 the Ceramiales was assembled to investigate the placement of *Harveyella mirabilis* and  
190 *Leachiella pacifica*, within the Rhodomelaceae (Salomaki et al. 2015, Verbruggen and  
191 Costa 2015, Hughey and Boo 2016, Díaz-Tapia et al. 2017). Shared plastid genes were  
192 extracted into 19 distinct datasets in Geneious Pro v. 9.1.5 (Kearse et al. 2012). The  
193 protein coding gene datasets were independently aligned using the translation align  
194 setting in Geneious v. 9.1.5 and the rRNAs were aligned using the MAFFT online server  
195 (Kato et al. 2017) and subsequently concatenated using Sequence Matrix v. 1.7.8  
196 (Vaidya et al. 2011) producing a 15,763 site dataset. The best-fit partitioning scheme and  
197 the best model of evolution for each partition was inferred using the Bayesian  
198 information criterion (BIC) as implemented in PartitionFinder2 (Lanfear et al. 2017). The  
199 concatenated dataset was then subjected to phylogenetic analysis using maximum  
200 likelihood, implemented in both RAxML v. 8.2.2 (Stamatakis 2014) and IQ-TREE v.  
201 1.5.6 (Nguyen et al. 2015), as well as Bayesian Inference using MrBayes v. 3.2.2

202 (Ronquist et al. 2012). For the maximum likelihood analysis the bootstrap support values  
203 were calculated using 1,000 bootstrap replicates in RAxML, and 1,000 replicates of  
204 ultrafast bootstrapping (UFBoot) in the IQ-TREE analysis (Hoang et al. 2018). For the  
205 Bayesian inference analysis, two Metropolis-coupled Markov chain Monte Carlo  
206 (MCMCMC) runs consisting of one cold chain and three hot chains were  
207 preformed. Each run was sampled every 500 generations for 2,000,000  
208 generations. After confirming the runs converged by checking to ensure that the average  
209 standard deviation of split frequencies was below 0.01, the trees were merged. The  
210 resulting tree and posterior probabilities were calculated from the 8,002 trees generated.

211

## 212 **RESULTS**

### 213 *An Exclusively Parasitic Clade*

214 Phylogenetic analysis was conducted on a concatenated dataset comprised of 19  
215 plastid-encoded genes from 54 free-living species, and the parasites *C. polysiphoniae*, *H.*  
216 *mirabilis*, *L. pacifica*. A Bayesian inference analysis implemented in MrBayes and  
217 maximum likelihood analyses using both RAxML and IQ-TREE all recovered robust  
218 support for a topology similar to that recovered by Díaz-Tapia et al. (2017). The three  
219 parasites formed a clade with 1.0 posterior probability (BI), 100% bootstrap support in  
220 RAxML and 100% ultrafast bootstrap approximation (UFBoot) in IQ-TREE (Fig. 1).  
221 *Choreocolax polysiphoniae* was the earliest branching parasite with *H. mirabilis* and *L.*  
222 *pacifica* being recovered as sister taxa with 100% bootstrap support/1.0 posterior  
223 probability (Fig. 1).

224

225 *Taxonomic Considerations*

226 *Choreocolax polysiphoniae* was initially described by Reinsch (1875) from the  
227 Atlantic coast of North America as parasitic on *Polysiphonia fastigiata* (now *Vertebrata*  
228 *lanosa*). Specimens used in the phylogenetic analysis presented here (Fig. 1) were  
229 collected at Beavertail State Park in Jamestown, RI, USA infecting *Vertebrata lanosa* and  
230 are a strong match to the type description (Reinsch 1875). A representative voucher of *C.*  
231 *polysiphoniae* on its host *V. lanosa* (03304648) has been deposited at the New York  
232 Botanical Garden herbarium (NY). As the type collection cannot be located, we formally  
233 lectotypify *C. polysiphoniae* on image #49 accompanying the description in Reinsch  
234 (1875). Based upon the molecular analyses here, which resolved a monophyletic clade of  
235 parasitic red algae within the Rhodomelaceae (Fig. 1), we formally transfer *Choreocolax*  
236 to the Rhodomelaceae and recognize Choreocolacaceae as a synonym of this family. To  
237 adhere to the principle of monophyly, the genus *Harveyella*, based on the type and only  
238 species *H. mirabilis* and included in our analyses (Fig. 1), is also transferred to the  
239 Rhodomelaceae.

240

241 *Parasite Plastid Genomes*

242 The complete plastid genome of *Harveyella mirabilis* was assembled as a 90,654  
243 kb circular molecule with 322x coverage. The plastid genome has an overall AT content  
244 of 76.5% and contains 84 protein coding genes, 3 rRNAs, and 23 tRNAs (Fig. 2). Similar  
245 to the *Choreocolax polysiphoniae* plastid (Salomaki et al. 2015), all genes related to  
246 photosynthesis have been lost with the exception of *petF*, which is involved in electron  
247 transport in other metabolic pathways (Happe and Naber 1993, Jacobs et al. 2009). Genes

248 involved in transcription/translation and fatty acid, amino acid, protein, isoprene  
249 biosynthesis remain conserved. As in the *C. polysiphoniae* plastid, *gltB* appears to be a  
250 pseudogene. BLAST similarity searches are able to find conserved homology, however  
251 the presence of stop-codons throughout the region suggests that the gene is likely no  
252 longer capable of being completely translated.

253 Five contigs, comprising 40,895 bp of the *Leachiella pacifica* plastid genome,  
254 were assembled and annotated. These genomic pieces encode 24 complete protein-coding  
255 genes, 6 protein-coding gene fragments at the ends of contigs, the small and large rRNA  
256 subunits, and 12 tRNAs. Similar to *H. mirabilis* and *C. polysiphoniae*, no genes  
257 associated with photosynthesis were recovered from the incomplete *L. pacifica* plastid  
258 genome.

259

### 260 *Plastid Genome Comparisons*

261 A whole genome MAUVE alignment of nine representative free-living Florideophyceae  
262 plastid genomes, the *H. mirabilis* and *C. polysiphoniae* genomes, identified 13 locally  
263 collinear blocks in the *H. mirabilis* genome that aligned with the free-living plastids (Fig.  
264 3). There were no rearrangements or inversions in the *H. mirabilis* plastid genome when  
265 compared to photosynthetic Rhodomelaceae taxa. When aligning *H. mirabilis* to the *C.*  
266 *polysiphoniae* plastid genome, 11 locally collinear blocks were identified, and several  
267 genome inversions and rearrangements are evident (Fig. 4). Additionally, gene content  
268 varies slightly between the two parasite plastid genomes. *Harveyella mirabilis* retains  
269 *argB*, *carA*, *infB*, *rnz*, *rpl9*, *rpl17*, *rpl24*, *rpl32*, *rpl33*, *rpl34*, *rpoZ*, *rps18*, *rps20*, *ycf21*,  
270 which have all been lost in *C. polysiphoniae* (Table 1), while *C. polysiphoniae* maintains

271 copies of *dnaB* and *fabH* which have both been lost in the *H. mirabilis* plastid genome.

272

## 273 **DISCUSSION**

### 274 *Parasite Plastids*

275         The link between plastid origin in red algal parasites and their evolutionary  
276 relationship to their hosts may be central to our understanding of red algal parasite  
277 evolution. The *Harveyella mirabilis* plastid genome (Fig. 2) represents the second red  
278 algal parasite demonstrated to retain a reduced native plastid. Similar to *Choreocolax*  
279 *polysiphoniae*, the *H. mirabilis* plastid genome remains conserved for functions including  
280 amino acid, fatty acid, and protein biosynthesis, but has lost genes involved in building  
281 the light harvesting apparatus, photosystems I and II, and other photosynthesis related  
282 genes. The partial *Leachiella pacifica* plastid genome presented here also supports that  
283 hypothesis, although work remains to completely sequence its plastid genome.

284         The *H. mirabilis* plastid gene order, with the exception of the missing  
285 photosynthesis genes, is conserved when compared to plastids of free-living  
286 Rhodomelaceae species (Fig. 3). In contrast, the *C. polysiphoniae* plastid has undergone  
287 greater gene loss than the *H. mirabilis* plastid, and a substantial amount of genome  
288 reorganization (Fig. 4). *Harveyella mirabilis* retains 13 genes that have been lost from the  
289 *C. polysiphoniae* plastid (Table 1); *argB* and *carA*, which are involved in arginine  
290 biosynthesis processes, *rpoZ*, which promotes RNA polymerase assembly, nine  
291 ribosomal protein genes, and an uncharacterized hypothetical protein. In contrast, *C.*  
292 *polysiphoniae* retains copies of *dnaB*, which is involved in DNA replication, and *fabH*,  
293 which is involved in fatty acid biosynthesis, both of which have been lost in *H. mirabilis*.

294 Analysis of additional plastid genomes in this clade will provide greater insights into  
295 patterns of plastid genome evolution in red algal parasites.

296

### 297 *The Demise of Exclusively Parasitic Families*

298 Sturch (1926) initially described the Choreocolacaceae as a family of  
299 holoparasites, containing the genera *Choreocolax*, *Harveyella*, and *Holmsella*. However,  
300 more recent morphological investigation showed that *Holmsella* was related to the  
301 parasites *Gelidiocolax* and *Pterocladiphila*, and it was moved to the family  
302 Pterocladophilaceae in the Gracilariales (Fredericq and Hommersand 1990). Their  
303 observations were subsequently supported by molecular data generated with the specific  
304 aim of testing the phylogenetic affinities of parasites that Sturch had assigned to the  
305 Choreocolacaceae. This work demonstrated that *Holmsella australis* and *Holmsella*  
306 *pachyderma* formed a well-supported monophyletic clade within the Gracilariaceae  
307 (Zuccarello et al. 2004). Their molecular data also indicated that *Choreocolax* and  
308 *Harveyella* belonged in the Ceramiales, leading the authors to question whether the  
309 Choreocolacaceae should continue to be recognized (Zuccarello et al. 2004). However,  
310 their use of 18S sequence data was insufficient to resolve a monophyletic clade  
311 exclusively comprised of parasites. Other authors have also noted that species in  
312 *Choreocolax*, *Harveyella*, and *Leachiella* have features aligning them to the Ceramiales,  
313 but again, taxonomic affinities among the parasite species and within this order remained  
314 uncertain (Goff and Cole 1975, Kugrens 1982, Fredericq and Hommersand 1990). Our  
315 data confirm the findings of Zuccarello et al. (2004), placing *Choreocolax*, *Harveyella*  
316 and *Leachiella* within the Rhodomelaceae. Furthermore, the phylogeny utilizing

317 additional molecular markers provides strong support for a clade containing  
318 *Choreocolax*, *Harveyella* and *Leachiella* (Fig. 1), and supports the placing the  
319 Choreocolacaceae in synonymy with the Rhodomelaceae. Since their adoption by  
320 Feldmann and Feldmann (1958) the terms adelphoparasite and alloparasite have been  
321 used to describe parasites that infect hosts within their tribe/family, or in different  
322 tribes/families, respectively. The use of these terms has been questioned as molecular  
323 data have revealed that alloparasites, like adelphoparasites, infect close relatives rather  
324 than distantly related species (Zuccarello et al. 2004, Kurihara et al. 2010). To date, there  
325 is only one documented case of intrafamilial infections by red algal parasites that are  
326 supported by molecular systematics of host and parasite (Zuccarello et al. 2004). By  
327 placing the family Choreocolacaceae in synonymy with the Rhodomelaceae we are  
328 making steps to move away from a taxonomic definition for red algal parasites in favor of  
329 a biological distinction.

330

### 331 *A Biological Basis for Distinguishing Red Algal Parasites*

332 With more than 120 described parasites occurring across eight Florideophyceae  
333 orders (Salomaki and Lane 2014, Blouin and Lane 2015, Preuss et al. 2017, Preuss and  
334 Zuccarello 2018), red algae appear more able to transition from autotrophy to parasitic  
335 lifestyles than any other eukaryotic lineage. The data presented here place *Choreocolax*  
336 *polysiphoniae*, *Harveyella mirabilis*, and *Leachiella pacifica* firmly within the same  
337 family as their hosts, further supporting abandonment of the adelpho/allo- terms for  
338 differentiating two types of red algal parasites. However, differences between two groups  
339 of parasites remain, including their developmental patterns as they infect their hosts, and



340 the origins of organelles (Table 2). We believe that it is time to abandon the terms  
341 adelpho- and allopasite, which are based upon a taxonomic framework that is different  
342 today than it was when these terms were introduced. Instead we propose to distinguish  
343 red algal parasites by biological characteristics that can be easily tested using molecular  
344 techniques, the retention of a native plastid. Throughout the remainder of this manuscript  
345 we will use the term “archaeplastic” parasite to refer to those parasites that retain a native  
346 plastid (formerly most allopasites), and “neoplastic” parasite to discuss those that hijack  
347 a host plastid rather than retain their own copy (formerly adelphoparasites).

348

#### 349 *Developmental differences*

350 It had long been recognized that the association between parasitic red algae and  
351 their hosts was facilitated, at least in part, by the ability of red algae to form cell to cell  
352 fusions between adjacent, non-daughter cells, called secondary pit connections (Sturch  
353 1899, 1926, Feldmann and Feldmann 1958). With modern microscopy, the structure and  
354 formation of secondary pit connections between parasites and their hosts was determined  
355 (Kugrens and West 1973, Goff and Cole 1976a, Wetherbee and Quirk 1982a, 1982b,  
356 Wetherbee et al. 1984). Furthermore, these cell to cell fusions were proposed to serve as  
357 the mechanism by which nutrients are transported from the host to parasite cells  
358 (Wetherbee and Quirk 1982b). With the use of epifluorescence microscopy, Goff went on  
359 to establish their importance in the infection process by demonstrating that red algal  
360 parasites are able to transfer their nuclei and organelles into host cells via secondary pit  
361 connections (Goff and Coleman 1984, 1985, 1987a, Goff and Zuccarello 1994).

362           In addition to recognizing the role of secondary pit connections in the infection  
363 process, sophisticated microscopy advanced our understanding of how parasitic red algae  
364 spread throughout their hosts and characterized the host responses. In a groundbreaking  
365 series of manuscripts, Goff described in great detail the biology of *Harveyella mirabilis*  
366 (Reinsch) F. Schmitz et Reinke, including its development, structure, and nutrient  
367 acquisition from its host *Odonthalia floccosa* (Esper) Falkenberg (Goff and Cole 1973,  
368 1975, 1976a, 1976b, Goff 1976, 1979a, 1979b). These investigations provided a  
369 framework to more intimately understand the development and interactions of a range of  
370 red algal parasites.

371           Aside from the formation of secondary pit connections that initiate host infection,  
372 important differences in developmental patterns and their subsequent spread throughout  
373 the hosts have been observed between the two types of parasites (reviewed in Salomaki  
374 and Lane 2014, Freese and Lane 2017). First, archaeplastic parasites including  
375 *Choreocolax*, *Harveyella*, and *Holmsella*, spread throughout their hosts by producing  
376 mitotically dividing rhizoidal filaments that grow among host cells (Sturch 1899, 1926,  
377 Goff and Cole 1976a, Fredericq and Hommersand 1990). In contrast, the neoplastic  
378 parasites *Gracilariophila oryzoides*, *Gardneriella tuberifera*, and *Janczewska gardneri*,  
379 infect their host cells directly and spread from cell to cell, rarely creating their own  
380 rhizoidal filaments (Goff and Coleman 1987a, Goff and Zuccarello 1994). Additionally,  
381 while neoplastic parasites appear to transform infected host cells and undergo nuclear  
382 replication solely within host cells (Goff and Coleman 1987a, Goff and Zuccarello 1994),  
383 archaeplastic parasites appear to only undergo DNA replication in their rhizoidal  
384 filaments and infected host cells maintain a 1:1 ratio of parasite nuclei to secondary pit

385 connections (Goff and Coleman 1984, 1985, 1987b). These key developmental  
386 differences further lend support for a means of discussing parasitic red algae in a  
387 biological rather than a taxonomic context.

388

### 389 *Organellar Origins*

390         The combination of microscopy with molecular tools challenged the dogma of  
391 how red algal parasites interact with their hosts. In a study investigating the origins of  
392 organelles from three neoplastic parasites, *Gracilariophila oryzoides*, *Gardneriella*  
393 *tuberifera*, and *Plocamiocolax pulvinata*, Goff and Coleman (1995) demonstrated that the  
394 parasites retain their own mitochondria. However all three had lost their native plastid,  
395 and instead incorporate a dedifferentiated host plastid when packaging their spores.  
396 Subsequent investigations into parasite mitochondria also implicated gene loss in the  
397 adelphoparasites *Gracilariophila oryzoides* and *Plocamiocolax pulvinata* (Hancock et al.  
398 2010). In their study, *atp8* and *sdhC* were described as pseudogenes in the *G. oryzoides*  
399 mitochondrion and *atp8* was noted as missing completely from the *P. pulvinata*  
400 mitochondrion genome (Hancock et al. 2010). These losses were attributed to decreased  
401 selective pressures as the parasites increasingly relied on their hosts for ATP and other  
402 molecules essential to their survival. A more recent investigation spurred by those results,  
403 demonstrated that gene loss in the parasite mitochondria were the result of sequencing  
404 errors and/or downstream analysis (Salomaki and Lane 2016).

405         Red algal parasite plastids appear to be more dynamic and perhaps the more  
406 interesting story in red algal parasite evolution. Molecular investigations including deep  
407 genomic sequencing, have confirmed that all adelphoparasites investigated to date,

408 *Faucheocolax attenuata*, *Gracilariophila oryzoides*, *Gardneriella tuberifera*,  
409 *Janczewska gardneri*, and *Plocamiocolax pulvinata* do not retain a native plastid (Goff  
410 and Coleman 1995, Salomaki and Lane, unpublished). Previously, the plastid genome has  
411 been completely sequenced from the archaeoplastic parasite *Choreocolax polysiphoniae*  
412 (Salomaki et al. 2015), and here we present the plastid genome of *Harveyella mirabilis*,  
413 and partial plastid genome sequences of *Leachiella pacifica*. Both completely sequenced  
414 plastids are greatly reduced in coding capacity compared to the plastids of free-living  
415 photosynthetic red algae, having lost all genes related to photosynthesis (Salomaki et al.  
416 2015). Interestingly, genes involved in amino acid and fatty acid biosynthesis, iron-sulfur  
417 cluster synthesis, as well as transcription and translation are conserved (Salomaki et al.  
418 2015). Aside from the loss of photosynthesis genes, the *H. mirabilis* plastid retains a high  
419 level of synteny with plastids of closely related free-living red algae, however the *C.*  
420 *polysiphoniae* plastid has experienced extensive genome reorganization (Figs. 3 & 4).

421         Developmental differences are notable, including the location of parasite DNA  
422 replication and mechanism of spreading throughout the host, but plastid origin appears to  
423 be central to differences observed in red algal parasite evolution. We hypothesize that the  
424 observed developmental differences between the traditionally termed adelpho- and  
425 alloparasites are intimately linked to plastid origin. Parasites that maintain a native plastid  
426 are, in essence, a complete red alga in their own right, while those that incorporate a host  
427 derived plastid are being pieced together with organelles from another organism they  
428 remain compatible with. By retaining their own plastid, the plastid remains under the  
429 same selective pressures as the rest of the parasite genome, and therefore, retains its  
430 ability to function for amino acid, fatty acid, protein, and isoprene biosynthesis – all

431 necessary functions for survival. Those parasites that retain their own plastid are  
432 therefore capable of developing and functioning similar to other free-living red algae,  
433 with the exception of not being able to photosynthesize. Furthermore, the maintenance of  
434 a native plastid and the resulting self-reliance would enable those parasites to endure  
435 through evolutionary time, successfully adapting to new hosts and speciating. This  
436 hypothesis can be tested in future studies by investigating the organellar origins of  
437 parasites in the genus *Holmsella*. *Holmsella pachyderma* was previously placed in the  
438 Choreocolacaceae based upon its developmental patterns within its host, until 1990 when,  
439 along with *Holmsella australis*, it was transferred to the Gracilariaceae based upon  
440 morphological characteristics (Fredericq and Hommersand 1990). A subsequent  
441 phylogenetic analysis including *H. australis* and *H. pachyderma* found that the species  
442 formed a monophyletic clade within the Gracilariaceae (Zuccarello et al. 2004). To date  
443 no work has been completed on the plastid origin of members of the genus *Holmsella*, but  
444 if they do retain a native plastid, *Holmsella* would represent a second successful  
445 evolution of parasites retaining archaeoplastic characteristics: a native plastid, mitotically  
446 dividing rhizoidal filaments as a means of vegetative growth throughout their hosts, and  
447 forming a monophyletic clade of parasite species. Further investigation of the taxonomic  
448 affiliation of parasite genera in families outside the Rhodomelaceae including  
449 *Gelidiocolax* and *Pterocladophila* is warranted.

450

#### 451 *Origin of Parasites*

452 Two hypotheses have been proposed for the origin of red algal parasites. Setchell  
453 (1918) suggested that a mutation in a spore causes parasites to arise sympatrically,

454 whereas Sturch (1926) postulated that parasitic red algae start out as epiphytes that  
455 become endophytes over time and increasingly rely on the host for nutrition. It seems  
456 plausible that Setchell's origin hypothesis could explain the rise of the neoplastic  
457 parasites, which comprise the majority of known red algal parasite biodiversity. By  
458 evolving from their hosts, neoplastic parasites could more easily incorporate a copy of a  
459 genetically similar plastid as their own. The adaptation of incorporating a host plastid  
460 may provide a quick fix for what otherwise would have been a lethal mutation. The  
461 unique parasite nucleus and mitochondrion could continue spreading from cell to cell of  
462 its newly acquired host (and savior) via secondary pit connections, essentially  
463 transforming the host cells as has been described (Goff and Coleman 1985, Goff and  
464 Zuccarello 1994). Although providing a means of short-term survival for the newly  
465 transitioned parasite, co-opting a host plastid as their own would also establish these  
466 parasites on an irreversible path towards their own extinction. In order for a non-  
467 photosynthetic parasite to survive it must retain compatibility for other plastid functions,  
468 including amino acid and fatty acid biosynthesis. Our current understanding suggests that  
469 the host-derived plastid is newly acquired during each new infection, therefore, the host  
470 plastid experiences one set of evolutionary pressures while the parasite nucleus evolves  
471 and accumulates mutations of its own. Eventually the parasite will inevitably lose the  
472 ability to communicate with the host plastid as the parasite and host increasingly become  
473 genetically distinct. This leaves the parasite with two possibilities, either find another  
474 host with a compatible plastid or go extinct. Alternatively, the success of an archaeoplastic  
475 parasite may be explained by Sturch's hypothesis. By evolving from a closely related  
476 epiphyte that is able to create secondary pit connections, the parasite may retain its own

477 plastid and therefore increase its longevity and the opportunity to speciate as the parasite  
478 adapts to new hosts. Therefore, what were previously viewed as competing hypotheses to  
479 explain the evolution of red algal parasites, may each explain how different types of  
480 parasites arose.

481

#### 482 *Conclusion*

483       Following the earliest investigations of red algal parasites, two groups were  
484 recognized based on morphological distinctions and they were initially separated by  
485 taxonomic affiliation with their hosts (Setchell 1918, Feldmann and Feldmann 1958, Goff  
486 1982). The use of molecular phylogenetics for evaluating evolutionary relationships has  
487 altered the taxonomic framework that was originally used for distinguishing red algal  
488 parasites. Distinct differences remain, however, and whether or not the parasite retains a  
489 native plastid or incorporates one from its host appears to be fundamental to parasite  
490 biology. We propose that the terminology for discriminating between red algal parasites  
491 should to reflect these biological differences, and identifying the plastid source has  
492 become substantially easier with modern sequencing technologies. Therefore, we  
493 recommend applying the term archaeoplastic parasite to describe those that retain a native  
494 plastid throughout the infection cycle, and neoplastic parasite to those that have lost their  
495 native plastid and instead incorporate a host plastid. We predict that investigations of  
496 parasites that have traditionally been referred to as alloparasites in families other than the  
497 Rhodomelaceae, like *Holmsella* and *Pterocladophila*, will also provide evidence of  
498 plastid retention and monophyletic clades of parasites.

499

500 **ACKNOWLEDGEMENTS**

501 The authors thank Craig Schneider and Gary Saunders for conversation regarding  
502 taxonomy and names for distinguishing parasites. Jillian Freese is thanked for collecting  
503 specimens of *Harveyella mirabilis* and *Leachiella pacifica*, and Kristina Terpis for her  
504 support in the lab. Funding for this work was provided to by a Phycological Society of  
505 America Grant-in-Aid of Research to ES and by grant #1257472 from the National  
506 Science Foundation awarded to CL. This research is based in part upon work conducted  
507 using the Rhode Island Genomics and Sequencing Center, which is supported in part by  
508 the National Science Foundation (MRI Grant No. DBI-0215393 and EPSCoR Grant Nos.  
509 0554548 & EPS-1004057), the US Department of Agriculture (Grant Nos. 2002-34438-  
510 12688 and 2003-34438-13111), and the University of Rhode Island.

511

512 **LITERATURE CITED**

513 Blouin, N. & Lane, C. 2015. Red algae provide fertile ground for exploring parasite  
514 evolution. *Perspect. Phycol.* 3:11–9.

515 Broadwater, S. T. & LaPointe, E. a 1997. Parasitic interactions and vegetative  
516 ultrastructure of *Choreonema thuretii* (Corallinales, Rhodophyta). *J. Phycol.*  
517 33:396–407.

518 Darling, A. C. E., Mau, B., Blattner, F. R. & Perna, N. T. 2004. Mauve□: Multiple  
519 alignment of conserved genomic sequence with rearrangements. *Genome Res.*  
520 14:1394–403.

521 Díaz-Tapia, P., Maggs, C. A., West, J. A. & Verbruggen, H. 2017. Analysis of  
522 chloroplast genomes and a supermatrix inform reclassification of the



- 523 Rhodomelaceae (Rhodophyta). *J. Phycol.* 53:920–37.
- 524 Feldmann, G. & Feldmann, J. 1958. Recherches sur quelques Floridees parasites. *Rev.*  
525 *Gen. Bot.* 65:49–128.
- 526 Finn, R. D., Cogill, P., Eberhardt, R. Y., Eddy, S. R., Mistry, J., Mitchell, A. L., Potter,  
527 S. C. et al. 2015. The Pfam protein families database: towards a more sustainable  
528 future. *Nucleic Acids Res.* 44:D279–85.
- 529 Finn, R. D., Mistry, J., Tate, J., Cogill, P., Heger, A., Pollington, J. E., Gavin, O. L. et  
530 al. 2010. The Pfam protein families database. *Nucleic Acids Res.* 38:D211–22.
- 531 Fredericq, S. & Hommersand, M. 1990. Morphology and systematics of *Holmsella*  
532 *pachyderma* (Pterocladophilaceae, Gracilariales). *Br. Phycol. J.* 25:39–51.
- 533 Freese, J. M. & Lane, C. E. 2017. Parasitism finds many solutions to the same problems  
534 in red algae (Florideophyceae, Rhodophyta). *Mol. Biochem. Parasitol.* 214:105–11.
- 535 Goff, L. J. 1976. The biology of *Harveyella mirabilis* (Cryptonemiales, Rhodophyceae).  
536 V. Host responses to parasite infection. *J. Phycol.* 12:313–28.
- 537 Goff, L. J. 1979a. The biology of *Harveyella mirabilis* (Cryptonemiales, Rhodophyceae).  
538 VI. translocation of photoassimilated <sup>14</sup>C. *J. Phycol.* 15:82–7.
- 539 Goff, L. J. 1979b. The biology of *Harveyella mirabilis* (Cryptonemiales, Rhodophyceae).  
540 VII. Structure and proposed function of host penetrating cells. *J. Phycol.* 15:87–100.
- 541 Goff, L. J. 1982. The biology of parasitic red algae. *Prog. Phycol. Res.* 1:289–369.
- 542 Goff, L. J., Ashen, J. & Moon, D. 1997. The evolution of parasites from their hosts: A  
543 case study in the parasitic red alga. *Evolution (N. Y.)* 51:1068–78.
- 544 Goff, L. J. & Cole, K. M. 1973. The biology of *Harveyella mirabilis* (Cryptonemiales,  
545 Rhodophyceae). I. Cytological investigations of *Harveyella mirabilis* and its host,

- 546 *Odonthalia floccosa*. *Phycologia*. 12:237–45.
- 547 Goff, L. J. & Cole, K. M. 1975. The biology of *Harveyella mirabilis* (Cryptonemiales,  
548 Rhodophyceae). II. Carposporophyte development as related to the taxonomic  
549 affiliation of the parasitic red alga, *Harveyella mirabilis*. *Phycologia*. 14:227–38.
- 550 Goff, L. J. & Cole, K. M. 1976a. The biology of *Harveyella mirabilis* (Cryptonemiales,  
551 Rhodophyceae). III. Spore germination and subsequent development within the host  
552 *Odonthalia floccosa* (Cermiales, Rhodophyceae). *Can. J. Bot. Can. Bot.* 54:268–80.
- 553 Goff, L. J. & Cole, K. M. 1976b. The biology of *Harveyella mirabilis* (Cryptonemiales,  
554 Rhodophyceae). IV. Life history and phenology. *Can. J. Bot. Can. Bot.* 54:281–92.
- 555 Goff, L. J. & Coleman, A. W. 1984. Transfer of nuclei from a parasite to host. *Proc. Natl.*  
556 *Acad. Sci.* 81:5420–4.
- 557 Goff, L. J. & Coleman, A. W. 1985. The role of secondary pit connections in red algal  
558 parasitism. *J. Phycol.* 21:483–508.
- 559 Goff, L. J. & Coleman, A. W. 1987a. Nuclear transfer from parasite to host: A new  
560 regulatory mechanism of parasitism. *Ann. N. Y. Acad. Sci.* 503:402–23.
- 561 Goff, L. J. & Coleman, A. W. 1987b. The solution to the cytological paradox of  
562 isomorphy. *J. Cell Biol.* 104:739–48.
- 563 Goff, L. J. & Coleman, A. W. 1995. Fate of parasite and host organelle DNA during  
564 cellular transformation of red algae by their parasites. *Plant Cell*. 7:1899–911.
- 565 Goff, L. J., Moon, D. A., Nyvall, P., Stache, B., Mangin, K. & Zuccarello, G. C. 1996.  
566 The evolution of parasitism in the red algae: Molecular comparisons of  
567 adelphoparasites and their hosts. *J. Phycol.* 32:297–312.
- 568 Goff, L. J. & Zuccarello, G. C. 1994. The evolution of parasitism in red algae—cellular

- 569 interactions of adelphoparasites and their hosts. *J. Phycol.* 30:695–720.
- 570 Guiry, M. D. & Guiry, G. M. 2018. *AlgaeBase*. World-wide electronic publication,  
571 National University of Ireland, Galway. <http://www.algaebase.org>; searched on 03  
572 October 2018.
- 573 Hancock, L., Goff, L. J. & Lane, C. E. 2010. Red algae lose key mitochondrial genes in  
574 response to becoming parasitic. *Genome Biol. Evol.* 2:897–910.
- 575 Happe, T. & Naber, J. D. 1993. Isolation, characterization and N-terminal amino acid  
576 sequence of hydrogenase from the green alga *Chlamydomonas reinhardtii*. *Eur. J.*  
577 *Biochem.* 214:475–81.
- 578 Hoang, D. T., Chernomor, O., Von Haeseler, A., Minh, B. Q. & Vinh, L. S. 2018.  
579 UFBoot2: Improving the ultrafast bootstrap approximation. *Mol. Biol. Evol.* 35:518–  
580 22.
- 581 Hughey, J. R. & Boo, G. H. 2016. Genomic and phylogenetic analysis of *Ceramium*  
582 *cimbricum* (Ceramiales, Rhodophyta) from the Atlantic and Pacific Oceans supports  
583 the naming of a new invasive Pacific entity *Ceramium sungminbooi* sp. nov. *Bot.*  
584 *Mar.* 0:211–22.
- 585 Jacobs, J., Pudollek, S., Hemschemeier, A. & Happe, T. 2009. A novel, anaerobically  
586 induced ferredoxin in *Chlamydomonas reinhardtii*. *FEBS Lett.* 583:325–9.
- 587 Kanehisa, M., Sato, Y., Kawashima, M., Furumichi, M. & Tanabe, M. 2016. KEGG as a  
588 reference resource for gene and protein annotation. *Nucleic Acids Res.* 44:D457–62.
- 589 Katoh, K., Rozewicki, J. & Yamada, K. D. 2017. MAFFT online service: multiple  
590 sequence alignment, interactive sequence choice and visualization. *Brief. Bioinform.*  
591 1–7.

- 592 Kearsse, M., Moir, R., Wilson, A., Stones-Havas, S., Cheung, M., Sturrock, S., Buxton, S.  
593 et al. 2012. Geneious Basic: an integrated and extendable desktop software platform  
594 for the organization and analysis of sequence data. *Bioinformatics*. 28:1647–9.
- 595 Kugrens, P. 1982. *Leachiella pacifica*, gen. et sp. nov., a new parasitic red alga from  
596 Washington and California. *Am. J. Bot.* 123:306–19.
- 597 Kugrens, P. & West, J. A. 1973. The ultrastructure of an alloparasitic red alga  
598 *Choreocolax polysiphoniae*. *Phycologia*. 12:175–86.
- 599 Kurihara, A., Abe, T., Tani, M. & Sherwood, A. R. 2010. Molecular phylogeny and  
600 evolution of red algal parasites: A case study of *Benzaitenia*, *Janczewskia*, and  
601 *Ululania* (Ceramiales). *J. Phycol.* 46:580–90.
- 602 Lanfear, R., Frandsen, P. B., Wright, A. M., Senfeld, T. & Calcott, B. 2017.  
603 Partitionfinder 2: New methods for selecting partitioned models of evolution for  
604 molecular and morphological phylogenetic analyses. *Mol. Biol. Evol.* 34:772–3.
- 605 Nguyen, L. T., Schmidt, H. A., Von Haeseler, A. & Minh, B. Q. 2015. IQ-TREE: A fast  
606 and effective stochastic algorithm for estimating maximum-likelihood phylogenies.  
607 *Mol. Biol. Evol.* 32:268–74.
- 608 Preuss, M., Nelson, W. A. & Zuccarello, G. C. 2017. Red algal parasites: a synopsis of  
609 described species, their hosts, distinguishing characters and areas for continued  
610 research. *Bot. Mar.* 60:1–13.
- 611 Preuss, M. & Zuccarello, G. C. 2018. Three new red algal parasites from New Zealand:  
612 *Cladhymenia oblongifoliaphila* sp. nov. (Rhodomelaceae), *Phycodryis novae-*  
613 *zelandiaeaphila* sp. nov. (Delesseriaceae) and *Judithia parasitica* sp. nov.  
614 (Kallymeniaceae). *Phycologia*. 57:9–19.

- 615 Reinsch, P. F. 1875. *Contributiones ad Algologiam et Fungologiam*. Lipsiae, Nuremberg.  
616 61 pp.
- 617 Ronquist, F., Teslenko, M., van der Mark, P., Ayres, D. L., Darling, A., Höhna, S.,  
618 Larget, B. et al. 2012. MrBayes 3.2: efficient Bayesian phylogenetic inference and  
619 model choice across a large model space. *Syst. Biol.* 61:539–42.
- 620 Salomaki, E. D. & Lane, C. E. 2014. Are all red algal parasites cut from the same cloth?  
621 *Acta Soc. Bot. Pol.* 83:369–75.
- 622 Salomaki, E. D. & Lane, C. E. 2016. Red algal mitochondrial genomes are more  
623 complete than previously reported. *Genome Biol. Evol.* 48:evw267.
- 624 Salomaki, E. D., Nickles, K. R. & Lane, C. E. 2015. The ghost plastid of *Choroecolax*  
625 *polysiphoniae*. *J. Phycol.* 51:217–21.
- 626 Saunders, G. W. 1993. Gel purification of red algal genomic DNA: An inexpensive and  
627 rapid method for the isolation of polymerase chain reaction-friendly DNA. *J.*  
628 *Phycol.* 29:251–4.
- 629 Schattner, P., Brooks, A. N. & Lowe, T. M. 2005. The tRNAscan-SE, snoscan and  
630 snoGPS web servers for the detection of tRNAs and snoRNAs. *Nucleic Acids Res.*  
631 33:686–9.
- 632 Setchell, W. A. 1914. Parasitic Florideae I. *Univ. Calif. Publ. Bot.* 6:1–34.
- 633 Setchell, W. A. 1918. Parasitism among the red algae. *Proc. Am. Philisophical Soc.*  
634 57:155–72.
- 635 Setchell, W. A. 1918. Parasitism among red algae. *Proc. Am. Philisophical Soc.* 57:155–  
636 72.
- 637 Setchell, W. A. 1923. Parasitic Florideae II. *Univ. Calif. Publ. Bot.* 10:393–401.

- 638 Stamatakis, A. 2014. RAxML version 8: A tool for phylogenetic analysis and post-  
639 analysis of large phylogenies. *Bioinformatics*. 30:1312–3.
- 640 Sturch, H. H. 1899. *Harveyella mirabilis* (Schmitz & Reinke). *Ann. Bot.* 8:83–102.
- 641 Sturch, H. H. 1926. *Choreocolax polysiphoniae*, Reinsch. *Ann. Bot.* XL.
- 642 The UniProt Consortium. 2017. UniProt: the Universal Protein knowledgebase. *Nucleic*  
643 *Acids Res.* 45:D158–69.
- 644 Vaidya, G., Lohman, D. J. & Meier, R. 2011. SequenceMatrix: Concatenation software  
645 for the fast assembly of multi-gene datasets with character set and codon  
646 information. *Cladistics*. 27:171–80.
- 647 Verbruggen, H. & Costa, J. F. 2015. The plastid genome of the red alga *Laurencia*. *J.*  
648 *Phycol.* 51:586–9.
- 649 Wetherbee, R. & Quirk, H. 1982a. The fine structure of secondary pit connection  
650 formation between the red algal allopasite *Holmsella australis* and its red algal  
651 host *Gracilaria furcellata*. *Protoplasma*. 176:166–76.
- 652 Wetherbee, R. & Quirk, H. 1982b. The fine structure and cytology of the association  
653 between the parasitic red alga *Holmsella australis* and its red algal host *Gracilaria*  
654 *furcellata*. *Protoplasma*. 165:153–65.
- 655 Wetherbee, R., Quirk, H. M., Mallett, J. E. & Ricker, R. W. 1984. The structure and  
656 formation of host-parasite pit connections between the red algal allopasite  
657 *Harveyella mirabilis* and its red algal host *Odonthalia floccosa*. *Protoplasma*.  
658 73:62–73.
- 659 Zuccarello, G. C., Moon, D. & Goff, L. J. 2004. A phylogenetic study of parasitic genera  
660 placed in the family Choreocolacaceae (Rhodophyta). *J. Phycol.* 40:937–45.
- 661

662 Table 1. *Harveyella mirabilis* plastid genes and their function, which have been lost from  
663 the *Choreocolax polysiphoniae* plastid genome.

664

<b>Gene Name</b>	<b>Biological Process and Molecular Function</b>
<i>argB</i>	Amino acid biosynthesis; ATP binding, acetylglutamate kinase activity
<i>carA</i>	Pyrimidine metabolism; ATP binding, carbamoyl-phosphate synthase (glutamine-hydrolyzing) activity
<i>infB</i>	Translation; Translation initiation, GTP binding
<i>rpl9</i>	Translation; structural constituent of the 50S ribosome
<i>rpl17</i>	Translation; structural constituent of the 50S ribosome
<i>rpl24</i>	Translation; structural constituent of the 50S ribosome
<i>rpl32</i>	Translation; structural constituent of the 50S ribosome
<i>rpl33</i>	Translation; structural constituent of the 50S ribosome
<i>rpl34</i>	Translation; structural constituent of the 50S ribosome
<i>rpoZ</i>	Transcription; DNA binding
<i>rps18</i>	Translation; structural constituent of the 30S ribosome
<i>rps20</i>	Translation; structural constituent of the 30S ribosome
<i>ycf21</i>	Uncharacterized hypothetical protein

665

666

667 Table 2. Distinguishing features between Archaeoplastic and Neoplastic parasites.

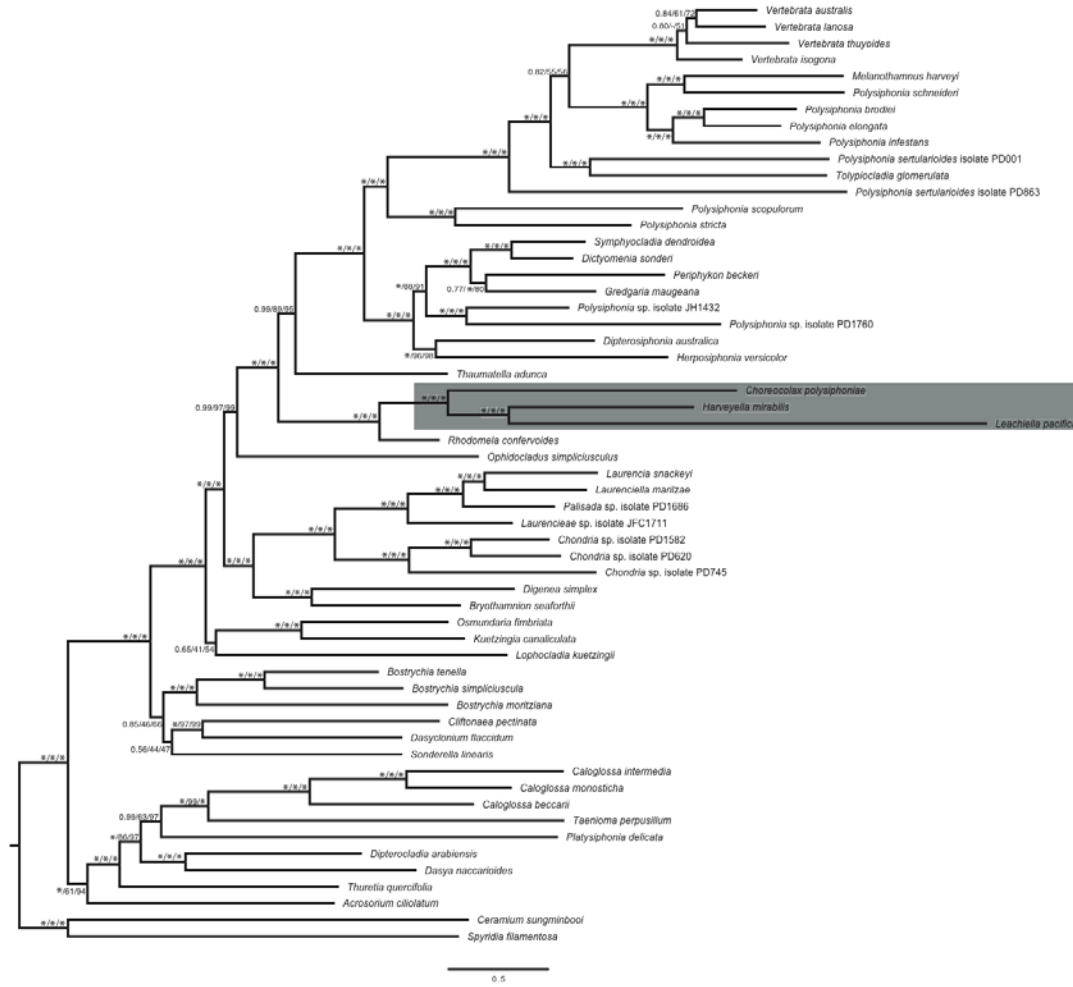
668

	Archaeoplastic parasites	Neoplastic parasites
Evolutionary origins	Monophyletic clades	Independent evolutionary events
Proliferation through host	Mitotically dividing rhizoidal filaments that directly fuse with host cells	Directly infect an individual host cell and subsequently spread from host cell to host cell via cell fusions
Site of nuclear DNA replication	Mitotically dividing parasite rhizoidal filaments	Host derived heterokaryon cells
Mitochondrion	Maintain complete and conserved native mitochondrion	Maintain complete and conserved native mitochondrion
Plastid	Retain a native plastid with reduced genetic capacity (loss of photosynthesis genes)	Utilize a host derived dedifferentiated plastid which is incorporated into parasite spores

669

670





671

672 **Figure 1.** Maximum likelihood phylogeny of the parasites *Choreocolax polysiphoniae*,  
673 *Harveyella mirabilis*, *Leachiella pacifica*, and 54 free-living members of the Ceramiales.

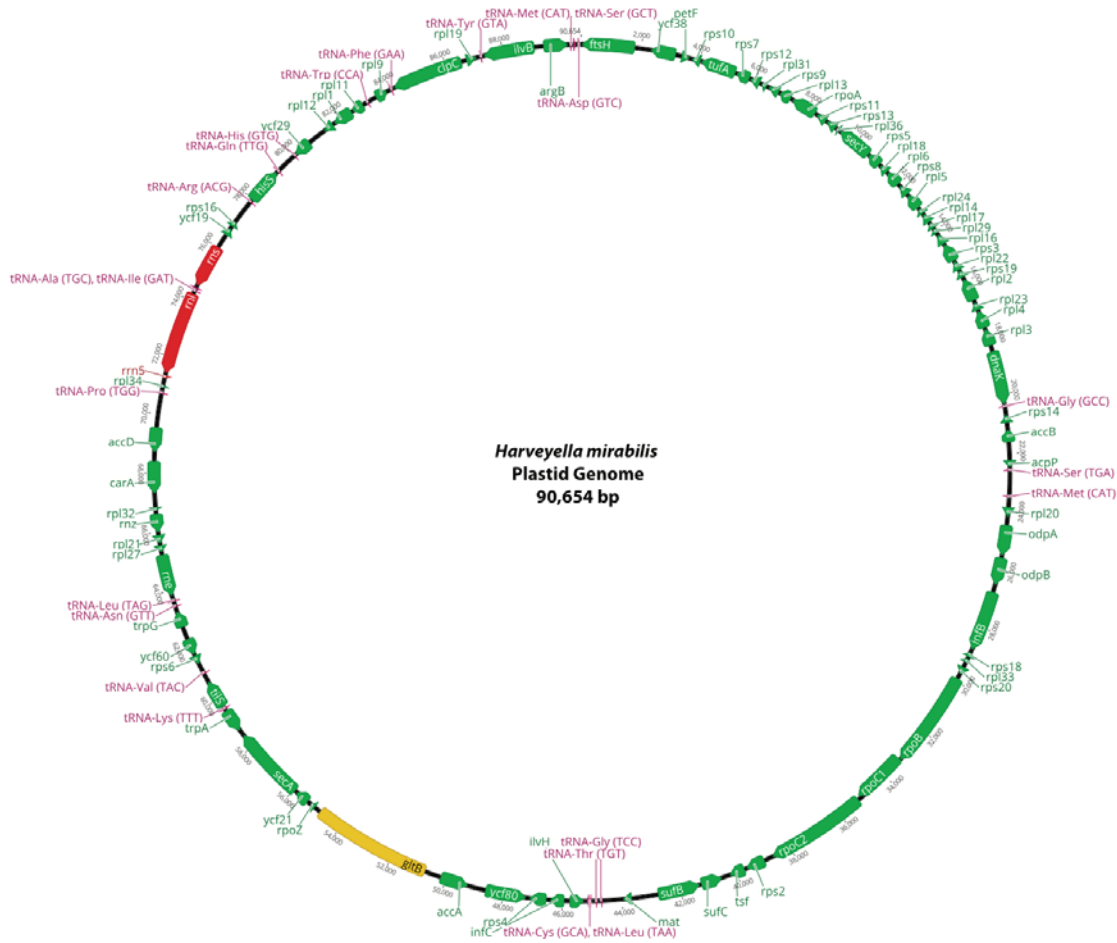
674 This analysis provides full support for a clade of parasites arising within the

675 Rhodomelaceae. Support values shown as Bayesian posterior probability/RAxML

676 bootstrap/IQ-TREE UFboot.

677

678

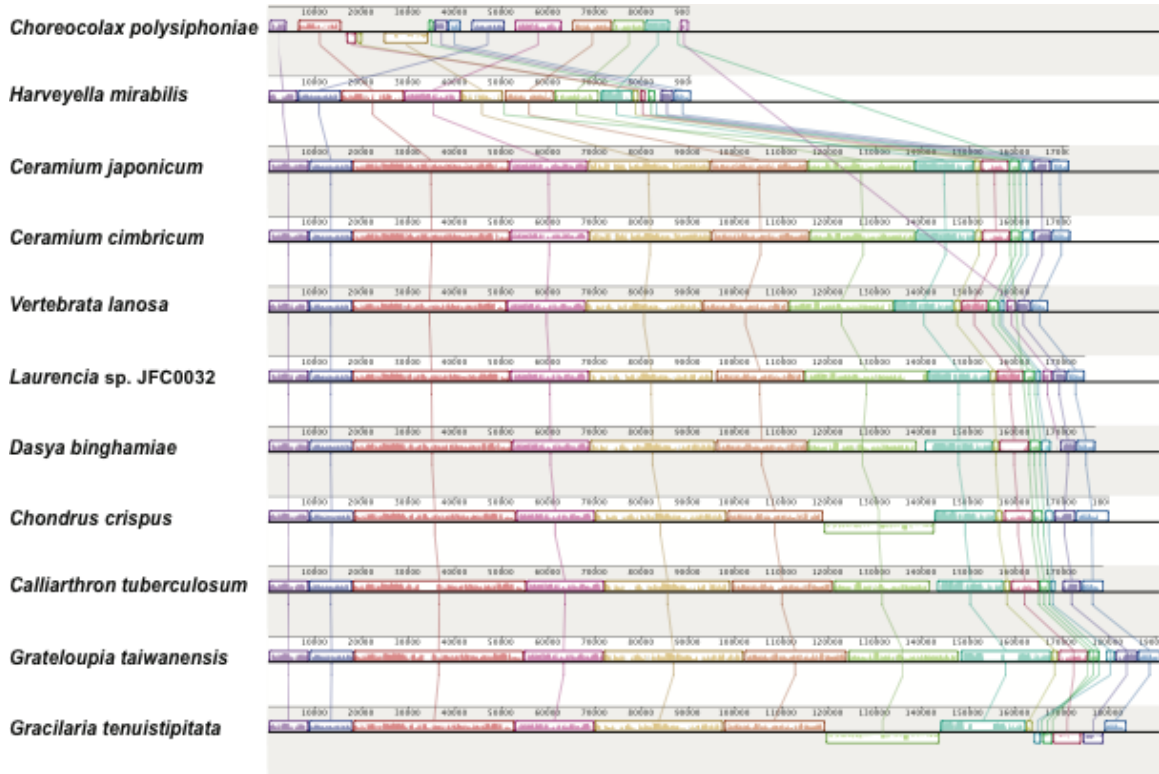


679

680 **Figure 2.** The plastid genome of the parasitic red alga, *Harveyella mirabilis* is 90,654  
 681 basepairs and contains 84 protein-coding genes (Green), the 5S, 16S, and 23S rRNAs  
 682 (Red), and 23 tRNAs (Pink). All genes involved with photosynthetic functions, except  
 683 *petF*, have been lost. The *ftsH* gene is truncated but may still be transcribed, however  
 684 *gliB* is a non-functional pseudogene (Yellow).

685

686

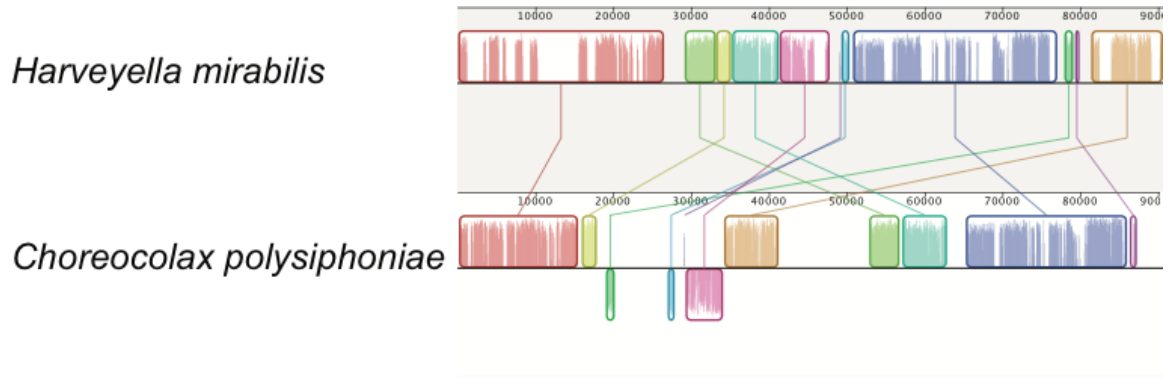


687

688 **Figure 3.** Mauve alignment of the parasites *Choreocolax polysiphoniae* (top) and  
689 *Harveyella mirabilis* (second from top) with all published Rhodomelaceae plastid  
690 genomes, as well as those from select representatives of other Florideophyceae families  
691 (*Dasya binghamiae*, Dasyaceae; *Chondrus crispus*, Gigartinaceae; *Calliarthron*  
692 *tuberculosum*, Corallinaceae; *Grateloupia taiwanensis*, Halymeniaceae; *Gracilaria*  
693 *tenuistipitata*, Gracilariaceae). This alignment identifies 16 locally collinear blocks  
694 (LCBs) among the selected plastid genomes and demonstrates that even with the loss of  
695 photosynthesis genes overall synteny is shared between the parasite *H. mirabilis* and  
696 other plastid genomes, while *C. polysiphoniae* has undergone several genome  
697 rearrangements.

698

699



700

701 **Figure 4.** Mauve alignment of the plastid genomes from the parasites *Harveyella*

702 *mirabilis* (top) and *Choreocolax polysiphoniae* (bottom). This alignment identifies 11

703 locally collinear blocks (LCBs) among these parasite plastid genomes, highlighting the

704 high level of genome fragmentation and rearrangements evident in the two parasite

705 plastids.

706